

Crystal Structures of Metallic and Insulating Molecular Complexes between Naphthaceno[5,6-*cd*:11,12-*c'd'*]bis[1,2]diselenole and 4,8-Bis(dicyanomethylene)-4*H*,8*H*-benzo[1,2-*c*:4,5-*c'*]bis[1,2,5]thiadiazole: (TSeN)(BTDA-TCNQ) and (TSeN)(BTDA-TCNQ)(C₆H₅Cl)

Kentaro IWASAKI,* Akito UGAWA, Atsushi KAWAMOTO, Yoshiro YAMASHITA, Kyuya YAKUSHI, Takanori SUZUKI,[†] and Tsutomu MIYASHI[†]

Department of Structural Molecular Science, The Graduate University for Advanced Studies, Institute for Molecular Science, Okazaki 444

[†]Department of Chemistry, Faculty of Science, Tohoku University, Sendai 980

(Received June 12, 1992)

The charge-transfer complex between naphthaceno[5,6-*cd*:11,12-*c'd'*]bis[1,2]diselenole (TSeN) and 4,8-bis(dicyanomethylene)-4*H*,8*H*-benzo[1,2-*c*:4,5-*c'*]bis[1,2,5]thiadiazole (BTDA-TCNQ) is found to show at least three different types of crystal modifications; insulating Type-I has a (1:1:1) ratio containing solvent molecules (chlorobenzene), metallic Type-II has a (1:1) stoichiometry, and semiconductive Type-III is conjectured to have a (1:2) or (2:1) stoichiometry. The crystal structures of Type-I and Type-II were determined by a single-crystal X-ray diffraction method. Type-I comprises mixed-stack molecular columns, and Type-II segregated-stack molecular columns. In both types the neighboring columns are linked along short molecular axes by two Se...N contacts that are shorter than the corresponding van der Waals contact. In the Type-II crystal, there are other short distances between TSeN and BTDA-TCNQ in the direction of the long molecular axes. From the C=C bond length in the C=C(CN)₂ group of BTDA-TCNQ, the degrees of charge transfer of these molecular complexes were estimated as 0.2±0.3 in Type-I and 0.9±0.2 in Type-II.

The electron acceptor, bis(1,2,5-thiadiazolo)tetra-cyanoquinodimethane (4,8-bis(dicyanomethylene)-4*H*,8*H*-benzo[1,2-*c*:4,5-*c'*]bis[1,2,5]thiadiazole, abbreviated as BTDA-TCNQ), was designed and synthesized by Yamashita et al. in order to improve the molecular property of 7,7,8,8-tetracyano-*p*-quinodimethane (TCNQ); first to decrease the on-site Coulomb energy by expanding the π -conjugated system, and second to increase the possibility of an inter-molecular interaction along the side-by-side direction by introducing sulfur atoms in the peripheral position of the molecule.¹⁾ Both of these properties are important factors regarding the design of a molecular metal. The first intention could be evidenced by decreasing the separation between the first and second redox potentials.¹⁾ The second one was actually found in several molecular complexes and anion radical salts of BTDA-TCNQ, which have inter-molecular short distances between the sulfur atoms of thiadiazole rings and the nitrogen atoms of the cyano groups. For example, the (TTF)(BTDA-TCNQ) complex has a sheet-like network through S...N≡C and S(TTF)...S(BTDA-TCNQ) contacts in addition to an alternately stacked column structure growing up perpendicular to this network plane, which is a characteristic of ordinary charge-transfer crystals (TTF=tetrathiafulvalene).²⁾ The anion radical salts of BTDA-TCNQ with alkylammonium cations prepared by Suzuki et al. show several stoichiometric ratios, i.e. (1:1), (2:3), (1:2), and (2:5).³⁾ In these crystals one-dimensionally stacked BTDA-TCNQs, are strongly linked by the inter-column S...N≡C bond. In the crystal of neutral BTDA-TCNQ, also, this molecule tends to make a 2-dimensional network through the same kind of S...N≡C bond.⁴⁾

To search for molecular metals, Yamashita et al. have prepared molecular complexes BTDA-TCNQ with tetrathionaphthacene (naphthaceno[5,6-*cd*:11,12-*c'd'*]bis[1,2]dithiole, abbreviated as TTN), TTF, TMTTF (tetramethyltetrathiafulvalene), and TMTSF (tetramethyltetraselenafulvalene), while considering the most appropriate oxidation potentials to realize a mixed-valence state⁵⁾ and expecting S...N≡C interactions to expand the dimensionality. Only the molecular complex with TTN showed a low resistivity (0.15 ohm cm at room temperature). This value of a powdered sample is even smaller than the resistivities of several single crystals of anion radical salts of BTDA-TCNQ.³⁾ Among these molecular complexes, the crystal structure is not known, except for the TTF complex, which has a mixed-stack structure. As for (TTN)(BTDA-TCNQ), nothing has been done, except for resistivity measurements on compacted pressed powders. Although we have not succeeded in growing a single crystal of (TTN)(BTDA-TCNQ), we have found that a single crystal of (TSeN)(BTDA-TCNQ) grown by a diffusion method shows a metallic behavior down to 1.5 K.⁶⁾ In this paper we describe the details concerning the crystal structure of this metallic crystal as well as another insulating crystal modification (TSeN)(BTDA-TCNQ)(C₆H₅Cl).

Experimental

Lustrous black needle (Type-I)- and plate (Type-II)-like crystals appear in the same batch of an H-shaped cell for a diffusion method. Single crystals began to appear after 3 weeks, and were harvested after 2 months when we used 50 ml of a chlorobenzene solution containing 5 mg of TSeN in one of the arms of an H-tube and 3 mg of BTDA-TCNQ in the other

Table 1. Crystal Data and Summary of Data Collection and Refinement Results

Modification	Type-I	Type-II
Compound	(TSeN)(BTDA-TCNQ)(C ₆ H ₅ Cl)	(TSeN)(BTDA-TCNQ)
Formula	C ₃₀ H ₈ N ₈ S ₂ Se ₄ · C ₆ H ₅ Cl	C ₃₀ H ₈ N ₈ S ₂ Se ₄
Formula weight/g mol ⁻¹	973.0	860.4
Cell parameters <i>a</i> /Å	12.025(5)	8.7149(4)
<i>b</i> /Å	13.839(6)	16.0795(6)
<i>c</i> /Å	7.598(4)	5.1937(2)
α /°	91.49(5)	95.772(3)
β /°	90.18(6)	99.258(4)
γ /°	139.17(2)	111.420(3)
Cell volume/Å ³	825.8(7)	658.57(5)
Formula unit number	1	1
Calculated density/g cm ⁻³	1.96	2.17
μ (Mo <i>K</i> α)/cm ⁻¹	45.41	55.93
<i>F</i> (0 0 0)	470	412
Space group	<i>P</i> $\bar{1}$	<i>P</i> $\bar{1}$
Crystal habit	Black needle	Black plate
Crystal size/mm	0.80×0.20×0.10	0.50×0.20×0.15
$2\theta_{\max}$ /°	50 (−14≤ <i>h</i> ≤14) (−16≤ <i>k</i> ≤16) (0≤ <i>l</i> ≤8)	55 (−11≤ <i>h</i> ≤11) (−21≤ <i>k</i> ≤21) (0≤ <i>l</i> ≤7)
Scan speed of ω /° min ⁻¹	6.0	6.0
Number of reflections		
[<i>F</i> _o >3 σ (<i>F</i> _o)]	2369	2338
Internal consistency	0.02	0.02
<i>R</i> (<i>R</i> _w)-factor	0.035 (0.039)	0.033 (0.038)
Goodness of fit	1.69	1.21
(Δ /σ) _{max}	0.80	0.14
$\Delta\rho_{\max}/\Delta\rho_{\min}$ /eÅ ⁻³	0.69/−0.48	0.80/−0.89

Table 2. Fractional Atomic Coordinates of Non-H Atoms and Their Equivalent Isotropic Thermal Parameters (Å²) with Estimated Standard Deviations in Parentheses. Equivalent Isotropic Thermal Parameter is Defined by $B_{eq} = (8/3)\pi^2 \sum \sum U_{ij} a_i^* a_j^* a_i \cdot a_j$.

Type-I					Type-II				
Atom	<i>x</i>	<i>y</i>	<i>z</i>	<i>B</i> _{eq}	Atom	<i>x</i>	<i>y</i>	<i>z</i>	<i>B</i> _{eq}
Se(1)	−0.33116(5)	−0.36715(4)	−0.16816(6)	4.31(2)	Se(1)	0.38070(4)	0.67614(2)	0.31392(7)	2.72(2)
Se(2)	−0.07023(5)	−0.27363(4)	−0.20684(5)	4.57(2)	Se(2)	0.41856(4)	0.59772(2)	−0.05336(7)	2.66(1)
C(1)	−0.5878(6)	−0.2651(5)	0.0384(7)	5.5(2)	C(1)	0.0006(5)	0.7027(3)	0.7802(7)	2.77(10)
C(2)	−0.4984(5)	−0.2838(4)	−0.0208(6)	4.5(2)	C(2)	0.1044(5)	0.6890(2)	0.6271(7)	2.32(9)
C(3)	−0.3176(5)	−0.1673(4)	−0.0043(5)	3.9(2)	C(3)	0.0431(4)	0.6175(2)	0.4058(6)	1.96(8)
C(4)	−0.2215(5)	−0.1845(4)	−0.0602(5)	3.9(2)	C(4)	0.1492(4)	0.6018(2)	0.2448(6)	1.95(8)
C(5)	−0.0442(4)	−0.0707(4)	−0.0410(5)	3.6(2)	C(5)	0.0880(4)	0.5298(2)	0.0291(6)	1.82(8)
C(6)	0.0520(5)	−0.0871(4)	−0.0978(5)	3.9(2)	C(6)	0.1930(4)	0.5140(2)	−0.1305(6)	2.02(8)
C(7)	−0.2299(6)	−0.0277(5)	0.0768(6)	4.1(3)	C(7)	−0.1316(4)	0.5589(2)	0.3478(6)	2.07(8)
C(8)	−0.3297(5)	−0.0131(5)	0.1349(6)	5.3(2)	C(8)	−0.2370(5)	0.5764(3)	0.5097(7)	2.65(10)
C(9)	−0.5032(5)	−0.1286(4)	0.1170(5)	6.2(2)	C(9)	−0.1719(5)	0.6459(3)	0.7190(8)	3.09(11)
S(1)	−0.1609(1)	−0.3137(1)	0.2869(1)	4.78(5)	S(1)	0.4367(1)	0.1000(1)	0.1266(2)	4.01(3)
N(1)	−0.2586(4)	−0.2825(3)	0.3573(4)	4.4(2)	N(1)	0.3063(4)	0.0233(2)	−0.1148(6)	3.16(9)
N(2)	0.0339(4)	−0.1561(3)	0.3385(4)	4.3(2)	N(2)	0.3070(4)	0.1184(2)	0.2911(6)	3.19(9)
C(10)	−0.1402(5)	−0.1454(4)	0.4295(5)	3.8(2)	C(10)	0.1520(4)	0.0081(2)	−0.0737(7)	2.32(9)
C(11)	0.0275(5)	−0.0730(4)	0.4189(5)	4.1(2)	C(11)	0.1523(4)	0.0633(2)	0.1605(7)	2.30(9)
C(12)	−0.1798(4)	−0.0779(4)	0.5129(5)	3.8(2)	C(12)	0.0003(4)	0.0588(2)	0.2463(6)	2.18(9)
C(13)	−0.3404(5)	−0.1473(4)	0.5228(5)	4.0(2)	C(13)	−0.0018(4)	0.1125(2)	0.4709(7)	2.26(9)
C(14)	−0.3810(5)	−0.0810(4)	0.5991(6)	4.8(2)	C(14)	0.1489(5)	0.1799(3)	0.6407(7)	2.74(10)
C(15)	−0.4921(5)	−0.2986(4)	0.4598(6)	4.8(2)	C(15)	−0.1498(5)	0.1101(3)	0.5599(7)	2.86(10)
N(3)	−0.4276(5)	−0.0397(4)	0.6559(5)	6.7(2)	N(3)	0.2591(4)	0.2350(2)	0.7887(7)	3.58(10)
N(4)	−0.6191(5)	−0.4141(4)	0.4156(6)	6.0(2)	N(4)	−0.2566(5)	0.1158(2)	0.6531(7)	4.05(11)
Cl(1)	0.0271(3)	0.6094(3)	0.1560(4)	7.7(2)					
C(16)	−0.1166(8)	0.3984(7)	0.3676(11)	9.4(4)					
C(17)	0.0113(7)	0.5487(7)	0.3397(9)	9.2(4)					
C(18)	0.1272(8)	0.6491(7)	0.4753(11)	8.4(4)					

arm. Slow cooling of a hot solution of TSeN and BTDA-TCNQ provided black tiny needles, which were characterized as Type-I from a comparison between the powder X-ray diffraction data and the single-crystal data. We obtained another modification (Type-III) when we used benzonitrile as the solvent in the diffusion method. Since the Type-III crystal does not have good quality, the cell parameters were determined by oscillation and Weissenberg photographs; monoclinic, $a=12.8$, $b=3.9$, $c=19.2$ Å, $\beta=94.0^\circ$, and $V=946$ Å³. The unit-cell volume is about 1.4-times larger than that of Type-II; we therefore suppose that the ratio of TSeN and BTDA-TCNQ is 1:2 or 2:1. We furthermore surmise that TSeN and BTDA-TCNQ are uniformly stacked on the basis of the short b -axis dimension. A preliminary experiment suggests that the Type-III crystal is semiconductive.

Determinations of the cell parameters and intensity collection were performed on a Rigaku AFC-5 four-circle diffractometer with graphite-monochromated MoK α radiation ($\lambda=0.71073$ Å). The unit-cell dimensions of Type-I and Type-II were determined using 16 ($37^\circ<2\theta<44^\circ$) and 20 ($20^\circ<2\theta<27^\circ$) reflections, respectively. During the intensity collection, three standard reflections were measured in every 100 reflections, showing no significant intensity decay. The structure was solved with the aid of a Monte-Carlo direct method⁷⁾ using the MULTAN78⁸⁾ program system. Atomic coordinates were refined by a full-matrix least-squares method. The minimized function was $\sum w(F_o - F_c)^2$, where a weighting scheme of $w=[\sigma^2(F_o)+0.00014F_o^2]^{-1}$ for Type-I and $w=[\sigma^2(F_o)]^{-1}$ for Type-II was used. All of the H atoms were found from the difference Fourier map and were refined with isotropic temperature factors equivalent to that of the bonded C atom. The crystal data, experimental condition for data collection, and results of the refinement are listed in Table 1. The atomic scattering factors were taken from "International Tables for X-Ray Crystallography."⁹⁾ All calculations were carried out on a Hitachi M-680 computer at the Institute for Molecular Science. ORTEP¹⁰⁾ was used to produce structure illustrations.

The atomic coordinates, except for those of the H atoms of Type-I and Type-II crystals, are given in Table 2. $F_o - F_c$ Tables; anisotropic temperature factors of Se, S, N, and C atoms, atomic coordinates and isotropic temperature factors of H atoms, bond lengths and angles involving H atoms of Type-I and Type-II crystals are deposited as Document No. 9046 at the Office of the Editor of Bull. Chem. Soc. Jpn.

Results and Discussion

Type-I: (TSeN)(BTDA-TCNQ)(C₆H₅Cl). Figure 1 shows the projection of the molecular arrangement along the c -axis and onto the $(1\bar{1}0)$ plane. TSeN and BTDA-TCNQ are alternately stacked, forming a mixed-stack molecular column along the c -axis. The molecular planes of TSeN and BTDA-TCNQ are almost parallel to each other, making, respectively, 26.2° and 27.7° with respect to the c -axis. The overlap pattern between TSeN and BTDA-TCNQ is shown in Fig. 2. The mean separation between these two planes is 3.40 Å. Within the molecular column, the shortest inter-molecular atomic distance is 3.379(5) Å for C(4)⋯N(1) (line a1), which is shorter than the sum (3.40 Å) of the van der Waals radii of C and N.^{11,12)} Other short ones are

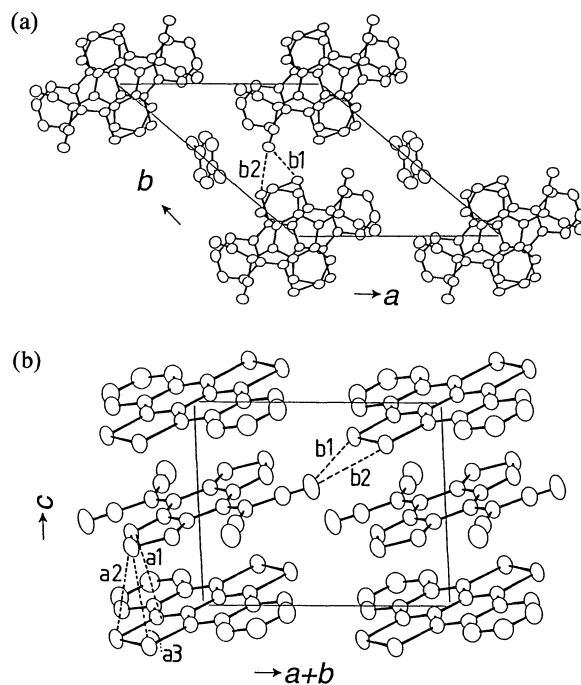


Fig. 1. Projection of the molecules (a) along c -axis and (b) onto the $(0\bar{1}1)$ plane in a Type-I crystal. The distances indicated by dotted lines are $a1=3.379(5)$, $a2=3.772(1)$, $a3=3.845(1)$, $b1=3.213(6)$, and $b2=3.165(6)$ Å.

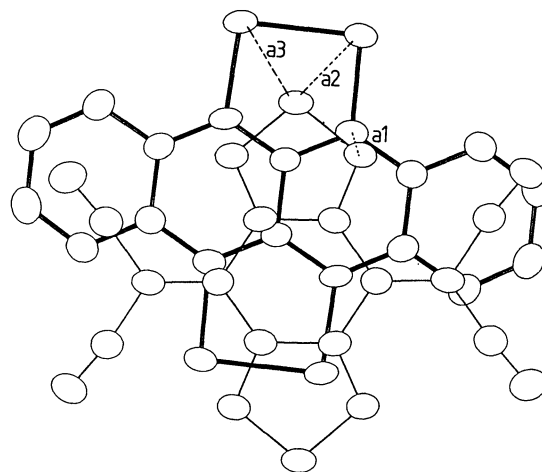


Fig. 2. Overlap pattern between TSeN and BTDA-TCNQ in the Type-I crystal. The distances indicated by dotted lines are $a1=3.379(5)$, $a2=3.772(1)$, and $a3=3.845(1)$ Å.

3.772(1) Å for Se(1)⋯S(1) (line a2) and 3.845(1) Å for Se(2)⋯S(1) (line a3), which are comparable to the sum of the van der Waals radii of S (1.80 Å) and Se (1.90 Å).¹¹⁾ Between different columns, on the other hand, there are Se⋯N distances which are significantly shorter than the van der Waals contact (3.30 Å);¹²⁾ the distance of Se(1ⁱ)⋯N(4ⁱⁱ) is 3.213(6) Å (line b1) and that of Se(2ⁱ)⋯N(4ⁱⁱ) is 3.165(6) Å (line b2), where [i] and [ii] represent the symmetry operation of $[-x, -y, -z]$ and

[1+x, 1+y, z]. The molecular columns, therefore, are linked by two Se and one N atoms. Since this linkage is extended along the [221] direction, the structure of this crystal comprises a sheet parallel to the (1 $\bar{1}$ 0) plane shown in Fig. 1(b). Between these sheets, solvent molecules, chlorobenzene, are included. This structural characteristics becomes more understandable by drawing the molecular array on (0 $\bar{1}$ 2) plane illustrated in Fig. 3. Since the chlorobenzene is located on the center of symmetry, the orientation of this molecule is disordered. Preliminary results concerning the polarized reflectance spectrum show that the charge-transfer band between TSeN and BTDA-TCNQ appears only along the *c*-axis. This means that the overlap of the HOMO of TSeN and LUMO of BTDA-TCNQ along the [221] direction is much smaller than that along the *c*-direction.

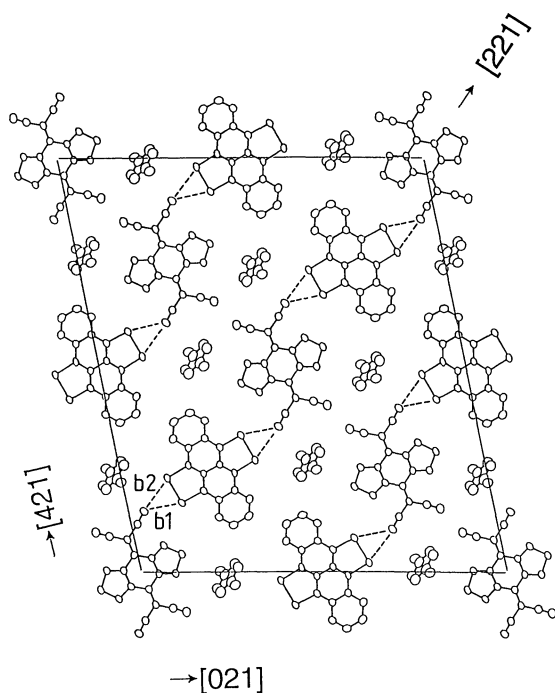


Fig. 3. Arrangement of molecules on the (0 $\bar{1}$ 2) plane in the Type-I crystal.

Both of molecules are planar with maximum out-of-plane distances of 0.016 Å for C(3) and C(6) in TSeN and 0.026 Å for N(1) in BTDA-TCNQ. Figure 4 shows the bond lengths of TSeN, BTDA-TCNQ, and chlorobenzene, the former two of which have approximately the *D*_{2h} symmetry. Suzuki et al. systematically analyzed the crystal structure of BTDA-TCNQ and its anion

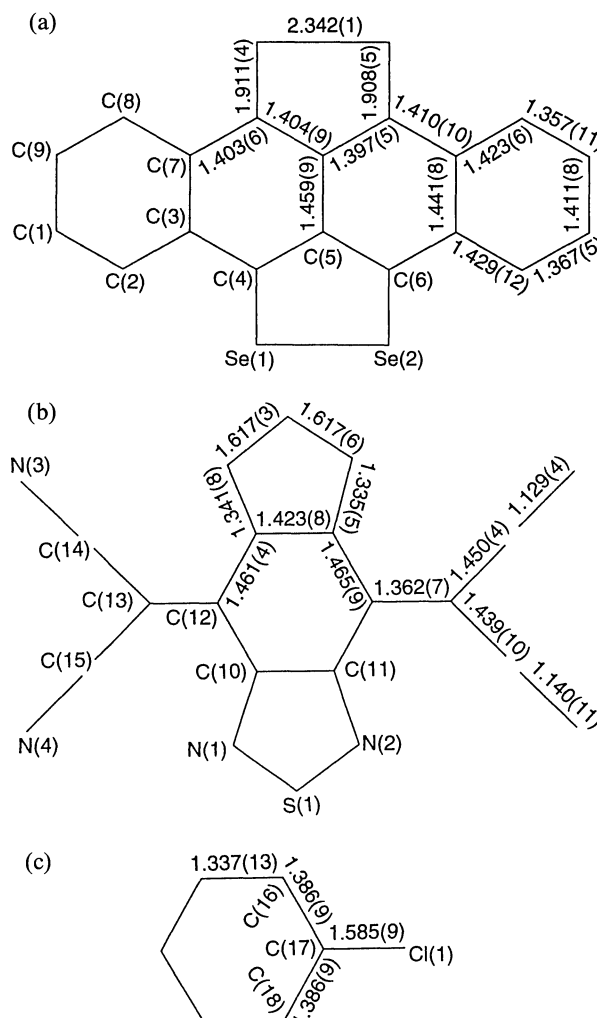


Fig. 4. Bond lengths of (a) TSeN, (b) BTDA-TCNQ, and (c) Chlorobenzene in Type-I crystal.

Table 3. Mean Values of Chemically Equivalent Bond Lengths (Å)

Bond	-1 ^{a)}	-0.5 ^{b)}	-0.5 ^{c)}	-0.5 ^{c)}	0.0 ^{d)}	Type-I ^{e)}	Type-II ^{e)}
a	1.614(4)	1.612(6)	1.615(8)	1.615(9)	1.617(6)	1.617(5)	1.611(4)
b	1.346(6)	1.340(8)	1.34(1)	1.34(1)	1.330(4)	1.338(7)	1.333(5)
c	1.433(5)	1.422(8)	1.43(1)	1.43(1)	1.422(6)	1.423(8)	1.431(5)
d	1.437(6)	1.449(8)	1.45(1)	1.45(1)	1.457(6)	1.463(7)	1.458(5)
e	1.390(6)	1.379(8)	1.37(1)	1.38(1)	1.356(7)	1.362(7)	1.387(5)
f	1.429(7)	1.42(1)	1.44(1)	1.43(1)	1.438(6)	1.445(7)	1.434(5)
g	1.140(6)	1.13(1)	1.13(1)	1.14(1)	1.143(5)	1.135(8)	1.142(5)

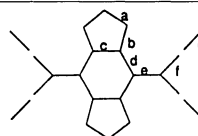
a) EtMe₃N⁺BTDA-TCNQ⁻ Ref. 3.

b) Bu₃MeN⁺(BTDA-TCNQ)₂⁻ Ref. 3.

c) Et₄N⁺(BTDA-TCNQ)₂⁻ Ref. 3.

d) BTDA-TCNQ Ref. 4.

e) This work.



radical salts,²⁾ and found a similar systematic geometrical change upon reduction, as in the case of TCNQ (tetracyanoquinodimethane). The mean bond lengths, assuming D_{2h} symmetry, are given in Table 3 for BTDA-TCNQ⁰, BTDA-TCNQ^{-0.5}, and BTDA-TCNQ⁻¹. In the case of TCNQ, a quinonoid structure of the neutral molecule changes into a benzenoid structure upon reduction, so that bonds **c**, **e**, and **g** are lengthened and, thus, bonds **d** and **f** are shortened.¹³⁾ As it is clear from Table 3, bonds **a**, **b**, **f**, and **g** do not change significantly, and only bonds **b** and **d**, and especially bond **e**, change significantly upon reduction. The reason why bonds **f** and **g** hardly change in BTDA-TCNQ is, perhaps, related to the existence of inter-molecular weak bonds between S or Se and N atoms, which were observed in all materials listed in Table 3. Incidentally, Yamashita et al. have claimed that the stretching frequency of the C≡N bond of BTDA-TCNQ is not systematically correlated to reduction, in contrast to the case of TCNQ.¹⁴⁾ They also consider this result as being the effect of inter-molecular S...N bonds. Since the change (0.034 Å) of bond **e** exceeds three times the standard deviation, and bond **e** of BTDA-TCNQ^{-0.5} is approximately positioned on a straight line between BTDA-TCNQ⁰ and BTDA-TCNQ⁻¹, by taking account of the standard deviation this bond length becomes the maker of the degree of charge transfer. The degree of charge transfer is, thus, estimated to be 0.2 ± 0.3 , assuming a linear relationship between the degree of charge-transfer and the bond-length change. The standard deviation is calculated using the propagation function of error. Finally, the bond angles of TSeN and BTDA-TCNQ are

given in Table 4 along with those of the Type-II crystal.

Type-II: (TSeN)(BTDA-TCNQ). Figure 5 shows a projection of the molecules along the *a*- and *c*-axes.

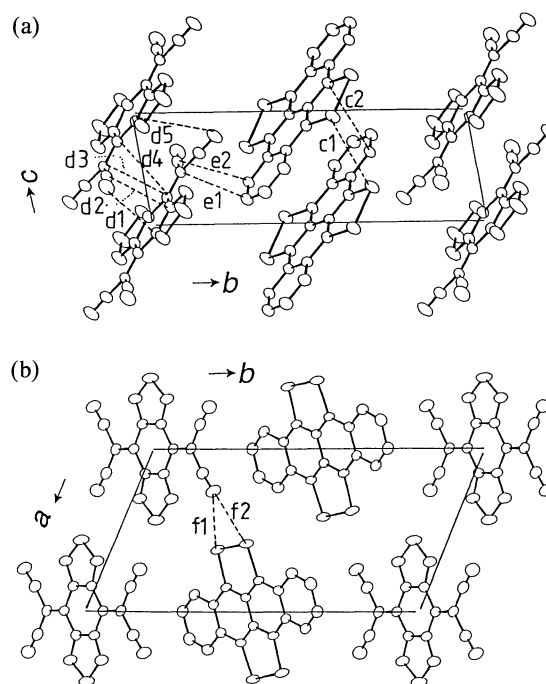


Fig. 5. Projection of the molecules along (a) the *a*-axis and (b) the *c*-axis in the Type-II crystal. The distances indicated by dotted lines are $c1=3.645(1)$, $c2=3.383(6)$, $d1=3.336(6)$, $d2=3.265(6)$, $d3=3.253(5)$, $d4=3.394$, $d5=3.270(6)$, $e1=3.370(6)$, $e2=3.360(6)$, $f1=3.098(4)$, and $f2=3.084(3)$ Å.

Table 4. Bond Angles (°) with esd's in Parentheses

Type I		Type II		Type I		Type II	
(a) TSeN		(a) TSeN		(b) BTDA-TCNQ		(b) BTDA-TCNQ	
Se(2)-Se(1)-C(4)	91.8(2)	Se(2)-Se(1)-C(4)	91.8(1)	N(1)-S(1)-N(2)	100.2(2)	N(1)-S(1)-N(2)	100.4(2)
Se(1)-Se(2)-C(6)	91.6(2)	Se(1)-Se(2)-C(6)	92.4(1)	S(1)-N(1)-C(10)	107.0(4)	S(1)-N(1)-C(10)	106.7(3)
C(2)-C(1)-C(9)	120.7(4)	C(2)-C(1)-C(9)	119.9(3)	S(1)-N(2)-C(11)	106.3(4)	S(1)-N(2)-C(11)	106.8(3)
C(1)-C(2)-C(3)	121.2(5)	C(1)-C(2)-C(3)	121.3(3)	N(1)-C(10)-C(11)	112.9(6)	N(1)-C(10)-C(11)	113.1(3)
C(2)-C(3)-C(4)	122.5(5)	C(2)-C(3)-C(4)	122.2(3)	N(1)-C(10)-C(12)	123.3(4)	N(1)-C(10)-C(12)	123.3(3)
C(2)-C(3)-C(7)	118.7(6)	C(2)-C(3)-C(7)	118.5(3)	C(11)-C(10)-C(12)	123.8(3)	C(11)-C(10)-C(12)	123.5(3)
C(4)-C(3)-C(7)	118.8(4)	C(4)-C(3)-C(7)	119.3(3)	N(2)-C(11)-C(10)	113.7(3)	N(2)-C(11)-C(10)	113.0(4)
C(3)-C(4)-C(5)	122.3(4)	C(3)-C(4)-C(5)	121.8(3)	N(2)-C(11)-C(12)	122.5(5)	N(2)-C(11)-C(12)	123.8(3)
Se(1)-C(4)-C(3)	120.5(2)	Se(1)-C(4)-C(3)	121.1(2)	C(10)-C(11)-C(12)	123.8(6)	C(10)-C(11)-C(12)	123.2(3)
Se(1)-C(4)-C(5)	117.1(5)	Se(1)-C(4)-C(5)	117.1(3)	C(10)-C(12)-C(11)	112.4(4)	C(11)-C(12)-C(10)	113.3(3)
C(4)-C(5)-C(6)	122.5(4)	C(4)-C(5)-C(6)	121.9(3)	C(13)-C(12)-C(11)	123.9(6)	C(11)-C(12)-C(13)	124.0(3)
C(4)-C(5)-C(5')	118.7(7)	C(4)-C(5)-C(5')	119.1(4)	C(10)-C(12)-C(13)	123.7(3)	C(13)-C(12)-C(10)	122.8(4)
C(6)-C(5)-C(5')	118.8(5)	C(6)-C(5)-C(5')	119.0(3)	C(12)-C(13)-C(14)	124.4(4)	C(12)-C(13)-C(14)	122.9(4)
C(5)-C(6)-C(7)	122.0(5)	C(5)-C(6)-C(7)	122.0(3)	C(12)-C(13)-C(15)	124.0(6)	C(12)-C(13)-C(15)	125.3(3)
Se(2)-C(6)-C(5)	117.0(2)	Se(2)-C(6)-C(5)	116.7(2)	C(14)-C(13)-C(15)	111.6(5)	C(14)-C(13)-C(15)	111.8(3)
Se(2)-C(6)-C(7)	120.9(5)	Se(2)-C(6)-C(7)	121.2(3)	N(3)-C(14)-C(13)	174.1(4)	N(3)-C(14)-C(13)	173.8(5)
C(3)-C(7)-C(6)	119.3(7)	C(3)-C(7)-C(6)	118.8(3)	N(4)-C(15)-C(13)	173.1(8)	N(4)-C(15)-C(13)	172.4(3)
C(3)-C(7)-C(8)	118.0(4)	C(3)-C(7)-C(8)	118.5(3)				
C(8)-C(7)-C(6)	122.7(5)	C(8)-C(7)-C(6)	122.7(3)	(c) Chlorobenzene			
C(7)-C(8)-C(9)	121.1(5)	C(7)-C(8)-C(9)	120.6(3)	C(17)-C(16)-C(18)	119.9(6)	C(17)-C(16)-C(18)	119.9(6)
C(8)-C(9)-C(1)	120.4(6)	C(8)-C(9)-C(1)	121.1(4)	C(16)-C(17)-C(18)	119.7(7)	C(16)-C(17)-C(18)	119.7(7)
				C(16)-C(17)-Cl(1)	121.4(5)	C(16)-C(17)-Cl(1)	121.4(5)
				C(18)-C(17)-Cl(1)	118.8(6)	C(18)-C(17)-Cl(1)	118.8(6)
				C(17)-C(18)-C(16)	120.3(6)	C(17)-C(18)-C(16)	120.3(6)

Each of the TSeN and BTDA-TCNQ is uniformly stacked so as to form a segregated-stack structure along the *c*-axis. The mean separations of TSeN and BTDA-TCNQ in each column are 3.323 and 3.257 Å, respectively. The molecular planes of TSeN and BTDA-TCNQ make angles of 53.6° and 56.9° with respect to the *c*-axis, respectively. Since their molecular planes are nearly parallel to each other, TSeN and BTDA-TCNQ are located on the same plane (1 $\bar{4}$ 1), as illustrated in Fig. 6. The overlap patterns of TSeN and BTDA-TCNQ are shown in Fig. 7. The overlap mode of TSeN resembles those of (TSeN)₂Cl¹⁵⁾ and (TTN)₂I₃¹⁶⁾ half of the molecules overlap with each other. Between these molecules, the inter-atomic distances of Se(1)···Se(2ⁱⁱⁱ)=3.645(1) Å (line c1) and C(1)···C(4ⁱⁱⁱ)=3.383(6) Å (line c2) are significantly shorter than the corresponding van der Waals contacts (3.80 Å and 3.40 Å), where [iii] represents the symmetry operation of [*x*, *y*, *z*+1]. The overlap mode of BTDA-TCNQ is different from what is known regarding the radical salts of BTDA-TCNQ.³⁾ Between these molecules there are five contacts shorter than 3.40 Å: C(10)···C(4^{iv})=3.336(6) Å (line d1), C(11)···C(15^{iv})=3.265(6) Å (line d2), C(12)···C(13^{iv})=3.253(5) Å (line d3), C(12)···C(12^{iv})=3.394(7) Å (line d4), and C(14)···C(10^{iv})=3.270(6) Å (line d5), where [iv] is the symmetry operation of [*-x*, *-y*, *1-z*]. Since TSeN and BTDA-TCNQ are remarkably shifted along the long molecular axes, as shown in Figs. 7(a) and (b), the cyano groups of BTDA-TCNQ on the (0, 0, 0) position overlap the peripheral benzene ring of TSeN located at the (0, 1/2, 1) position, as shown in Fig. 7(c). Between these molecules, there are two contacts shorter than 3.40 Å; C(13)···C(1ⁱⁱ)=3.370(6) Å (line e1) and C(15)···C(2ⁱⁱ)=3.360(6) Å (line e2). This kind of interchain overlap is reminiscent of

the spanning overlap in α -Et₂Me₂N[Ni(dmit)₂]₂, named by R. Kato et al.²¹⁾ This interaction extends along the [0 1 2] direction, as is shown in Fig. 5(a). Figure 8 is a comprehensive drawing of the spanning overlap which

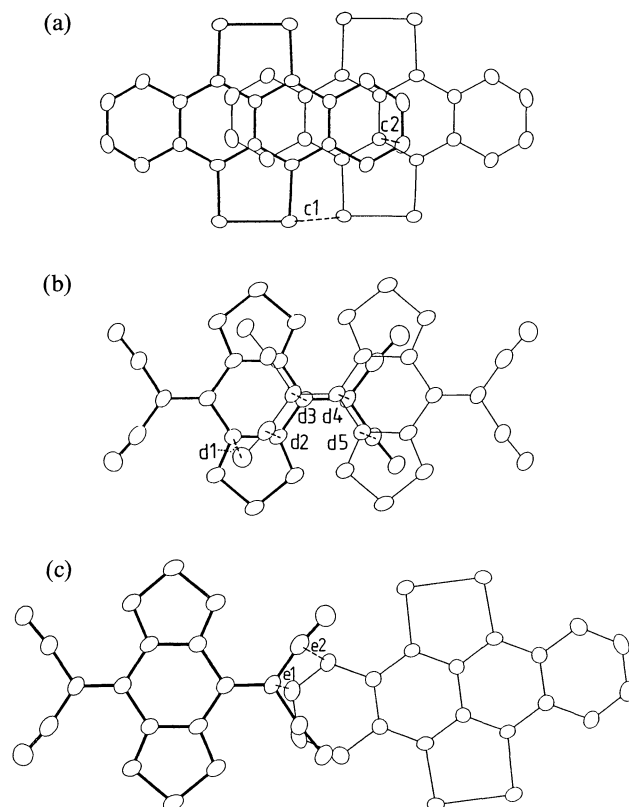


Fig. 7. Overlap patterns between (a) TSeN molecules, (b) BTDA-TCNQ molecules, and (c) TSeN and BTDA-TCNQ molecules. The distances indicated by dotted lines are c1=3.645(1), c2=3.383(6), d1=3.336(6), d2=3.265(6), d3=3.253(5), d4=3.394, d5=3.270(6), e1=3.370(6), and e2=3.360(6) Å.

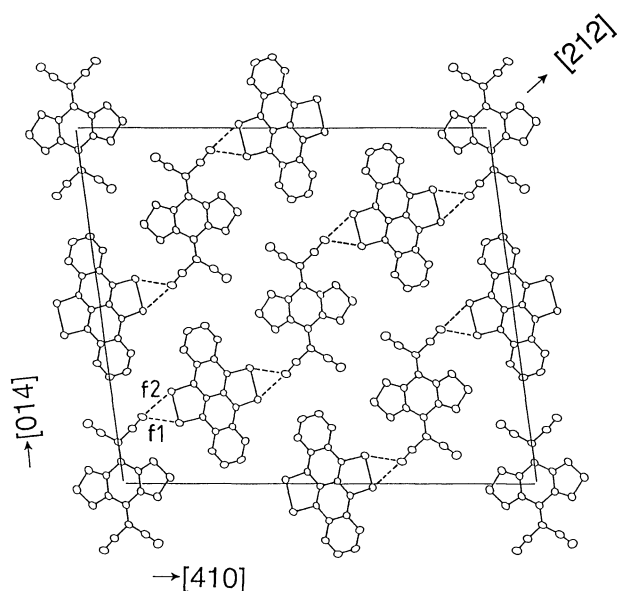


Fig. 6. Arrangement of molecules on the (1 $\bar{4}$ 1) plane in the Type-II crystal.

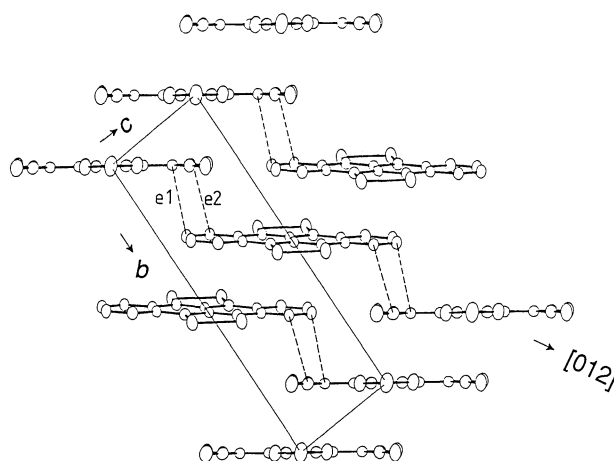


Fig. 8. Side view of TSeN and BTDA-TCNQ columns growing up along the *c*-axis. These columns are connected to each other by the spanning overlap indicated by the dotted lines, e1=3.370(6) and e2=3.360(6) Å.

spans the donor and acceptor columns. Between TSeN and BTDA-TCNQ, there are other remarkably short inter-column contacts, such as $\text{Se}(1) \cdots \text{N}(3^{\text{ii}}) = 3.098(4)$ Å (line f1) and $\text{Se}(2) \cdots \text{N}(3^{\text{ii}}) = 3.084(3)$ Å (line f2) shown in Figs. 5(b) and 6. This type of interaction is the same as that found in Type-I (lines b1 and b2); moreover, these distances are shorter than the corresponding values of the $\text{Se} \cdots \text{N}$ distances of Type-I. This $\text{Se} \cdots \text{N}=\text{C}$ linkage extends along the $[212]$ direction. As a result, the molecular columns of TSeN and BTDA-TCNQ are connected by a $p\sigma$ - $p\sigma$ type interaction along the $[012]$ direction, and by a $p\pi$ - $p\pi$ type interaction along the $[212]$ direction. If the frontier orbitals of donor and acceptor molecules in the adjacent columns mix strongly through these short atomic distances, that effect will appear in the optical spectrum. However, as we have already reported, Drude-like reflectivity appears only when the polarization of light is parallel to the c -axis, at least in the spectral region higher than 650 cm^{-1} .⁶⁾ This means that the conduction band is very anisotropic and that the $p\sigma$ - $p\sigma$ interaction between the HOMOs of neighboring TSeN or LUMOs of neighboring BTDA-TCNQ is much stronger than the other interactions along the $[012]$ or $[212]$ directions. This result is rather easily understandable, since the number of interacting atoms along the $[012]$ and $[212]$ directions is much smaller. Furthermore, the weak interaction of $\text{Se} \cdots \text{N}=\text{C}$, despite its very short distance, might be related to the anisotropy of the p -atomic orbitals that make π -molecular orbitals. The p -orbital is elongated perpendicular to the molecular plane; molecules which are connected by $\text{Se} \cdots \text{N}=\text{C}$ linkage, are in the same $(1\bar{4}1)$ plane as shown in Fig. 6. The overlap of the π -orbitals along the $[212]$ direction is expected to be much weaker. The same as well as more quantitative discussions have been made by Mori et al. concerning a variety of crystal modifications of BEDT-TTF (bis(ethylenedithio)tetrathiafulvalene) salts based on calculations of the overlap integrals of the HOMOs.¹⁷⁾ The anisotropic situation in Type-I described before is the same as in this case.

The TSeN and BTDA-TCNQ molecules are planar with maximum out-of-plane distances of 0.066 Å for $\text{Se}(2)$ and $\text{C}(6)$ in TSeN and 0.025 Å for $\text{N}(2)$ in BTDA-TCNQ. The bond lengths of TSeN and BTDA-TCNQ are shown in Fig. 9. The planarity and bond-length distribution show that TSeN and BTDA-TCNQ have approximately the D_{2h} symmetry. As shown in Table 3, bond length e , which is most sensitive to reduction, indicates that BTDA-TCNQ of a Type-II modification is close to an anionic structure. The degree of charge transfer estimated in the same way as for Type-I is 0.9 ± 0.2 . In the case of TTN, a sulfur analog of TSeN, S-S and S-C bonds tend to become shorter upon oxidation.^{16,18,19)} This geometrical relaxation is theoretically supported as well.²⁰⁾ The bond lengths of Se-Se and Se-C are $2.342(1)$ and $1.910(5)$ Å for Type-I and $2.315(1)$ and $1.883(3)$ Å for Type-II, respectively. If the

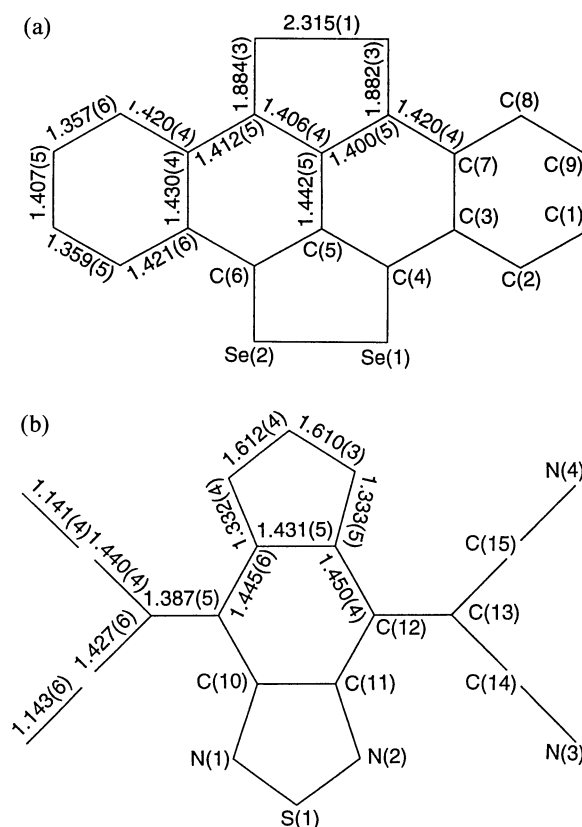


Fig. 9. Bond lengths of (a) TSeN and (b) BTDA-TCNQ in Type-II crystal.

same tendency is assumed in TSeN, this difference of the bond lengths between Type-I and -II is consistent with the conclusion that the Type-II crystal is much more ionic, the result of which was derived from bond length e of BTDA-TCNQ. Furthermore, the bond lengths of $\text{TSeN}^{+0.5}$ in $(\text{TSeN})_2\text{Cl}$ are $2.323(1)$ Å for Se-Se and $1.901(6)$ Å for Se-C.¹⁵⁾ These values are just between the corresponding values of Type-I ($\text{TSeN}^{+0.2(3)}$) and Type-II ($\text{TSeN}^{+0.9(2)}$). Consequently, our estimation of the degrees of charge transfer of Type-I and Type-II is again reasonable.

Finally, we give a comparison of the crystal structures of Type-I and Type-II, which appear to be quite different from each other at first glance. Comparing Figs. 3 and 6, the resemblance of the molecular arrays of Type-I and Type-II on these planes become clear, especially the patterns linked through the $\text{Se} \cdots \text{N}=\text{C}$ bonds extending along $[221]$ in Type-I and $[212]$ in Type-II are very similar to each other. If we take away the solvent molecules from the Type-I crystal and then slide the sheet in an appropriate direction, the structure of Type-I is converted to Type-II without any further large modification. This suggests that the $\text{Se} \cdots \text{N}=\text{C}$ bonds are retained in both modifications in spite of the fact that the π - π type overlap modes are entirely different. The molecular packing i.e. crystal lattice of $(\text{TSeN})(\text{BTDA-TCNQ})$ is probably ruled by the $\text{Se} \cdots \text{N}=\text{C}$ interaction and shape of molecule, although this interaction does

not strongly contribute to an interchain transfer of electrons. We have pointed out the possibility that this Se...N≡C bond plays a role in acting as a bridge which connects donor and acceptor stacks, and that this bridge resists a Peierls distortion along the stack.⁶⁾ This situation reminds us of the structure of Ag(DMe-DCNQI)₂,²²⁾ where the cyano group makes a coordination bond with the Ag atom so that an interchain bridge, such as C≡N...Ag...N≡C, is formed.²³⁾ In spite of this bridge, Ag(DMe-DCNQI)₂ has a one-dimensional electronic structure,²⁴⁾ which means that hybridization does not occur between the LUMO of DMe-DCNQI and 4d-orbitals of Ag. According to this one-dimensional electronic structure, this material shows a Peierls distortion.²⁵⁾ On one hand, the anisotropic band structure of (TSeN)(BTDA-TCNQ) Type-II crystal is quite similar to Ag(DMe-DCNQI)₂; on the other hand, the ground state is different in the sense that it does not undergo the Peierls transition. Consequently, we must take into account the spanning overlap along the [0 1 2] direction, which perhaps slightly modifies the one-dimensional Fermi surface, although it is not detected in the reflectance spectrum in regions higher than 650 cm⁻¹. It is not clear at this moment which interchain interactions mainly fill the role of suppressing the Peierls distortion. Low-temperature optical measurements in the far-infrared region should solve this problem.

Contrary to expectation, it was found that the sulfur atoms of BTDA-TCNQ do not participate in the interchain interaction. However, the linkage pattern of Se...N≡C shown in Figs. 3 and 6 might be realized by introducing thiadiazole rings that would modify the molecular shape of TCNQ. In this sense the selenium analog of BTDA-TCNQ may have the same crystal structure and thus may become the best candidate for a molecular metal, although we have not obtained a single crystal, because of its very low solubility to organic solvents.

In summary, we have found three different types of crystals in the molecular complexes between TSeN and BTDA-TCNQ. The insulating crystal, Type-I, has a mixed-stack structure, while the metallic crystal, Type-II, has a segregated-stack structure. In both modifications, TSeN and BTDA-TCNQ in the neighboring columns are connected by Se...N≡C, and the molecular arrays on the plane on which TSeN and BTDA-TCNQ are placed are quite similar to each other, despite the fact that the stacking modes are entirely different. In addition to this Se...N≡C interaction, there is another interchain interaction, a spanning overlap, in the Type-II crystal. From the molecular geometry, the degrees of charge-transfer are estimated to be 0.2±0.3 in Type-I

and 0.9±0.2 in Type-II.

References

- 1) Y. Yamashita, T. Suzuki, T. Mukai, and G. Saito, *J. Chem. Soc., Chem. Commun.*, **1985**, 1044.
- 2) T. Suzuki, C. Kabuto, Y. Yamashita, and T. Mukai, *Bull. Chem. Soc. Jpn.*, **60**, 2111 (1987).
- 3) T. Suzuki, C. Kabuto, Y. Yamashita, T. Mukai, T. Miyashi, and G. Saito, *Bull. Chem. Soc. Jpn.*, **61**, 483 (1988).
- 4) C. Kabuto, T. Suzuki, Y. Yamashita, and T. Mukai, *Chem. Lett.*, **1986**, 1433.
- 5) G. Saito and J. P. Ferraris, *Bull. Chem. Soc. Jpn.*, **53**, 2141 (1980).
- 6) A. Ugawa, K. Iwasaki, A. Kawamoto, Y. Yamashita, K. Yakushi, and T. Suzuki, *Phys. Rev. B*, **43**, 14178 (1991).
- 7) A. Furusaki, *Acta Crystallogr., Sect. A*, **35**, 220 (1979).
- 8) P. Main, S. E. Hull, L. Lessinger, G. Germain, J.-P. Declercq, and M. M. Woolfson, "MULTAN78, A System of Computer Programs for the Automatic Solution of Crystal Structures from X-Ray Diffraction Data," University of York, England, Louvain, Belgium (1978).
- 9) "International Tables for X-Ray Crystallography (1974)," Kynoch Press Birmingham, England, Vol. 4.
- 10) C. K. Johnson, ORTEP. Report ORNL-3794. Oak Ridge National Laboratory, Tennessee, USA (1965).
- 11) A. Bondi, *J. Phys. Chem.*, **68**, 441 (1964).
- 12) According to Ref. 11 the van der Waals radii of N atom of cyano group is quite anisometric: 1.4 Å parallel to the CN bond and 1.7 Å perpendicular to the bond.
- 13) T. C. Umland, S. Allie, T. Kuhlmann, and P. Coppens, *J. Phys. Chem.*, **92**, 6456 (1988).
- 14) Y. Yamashita, T. Suzuki, and T. Mukai, *J. Chem. Soc., Chem. Commun.*, **1987**, 1184.
- 15) R. P. Shibaeva and V. F. Kaminskii, *Sov. Phys. Crystallogr.*, **23**, 1183 (1978).
- 16) D. L. Smith and H. R. Luss, *Acta Crystallogr., Sect. B*, **33**, 1744 (1977).
- 17) T. Mori, A. Kobayashi, Y. Sasaki, H. Kobayashi, G. Saito, and H. Inokuchi, *Bull. Chem. Soc. Jpn.*, **57**, 627 (1984).
- 18) O. Dideberg and J. Toussaint, *Acta Crystallogr., Sect. B*, **30**, 2481 (1974).
- 19) R. P. Shibaeva, V. F. Kaminskii, O. N. Evyomenko, E. B. Yagubskii, and M. L. Khidkekel, *Sov. Phys. Crystallogr.*, **25**, 31 (1980).
- 20) J.-P. Boutique, J. Riga, J. J. Verbist, J. G. Fripiat, and J. Delhalle, *Mol. Cryst. Liq. Cryst.*, **101**, 175 (1983).
- 21) R. Kato, H. Kobayashi, H. Kim, A. Kobayashi, Y. Sasaki, T. Mori, and H. Inokuchi, *Chem. Lett.*, **1988**, 865.
- 22) DMe-DCNQI is the abbreviation of *N,N'*-dimethyl-2,5-dicyano-*p*-quinone diimine.
- 23) R. Kato, H. Kobayashi, A. Kobayashi, T. Mori, and H. Inokuchi, *Chem. Lett.*, **1987**, 1579.
- 24) K. Yakushi, A. Ugawa, G. Ojima, T. Ida, H. Tajima, H. Kuroda, A. Kobayashi, R. Kato, and H. Kobayashi, *Mol. Cryst. Liq. Cryst.*, **181**, 217 (1990).
- 25) R. Moret, *Synth. Met.*, **27**, B301 (1988).